# The First Mixed-Halide Zirconium Cluster Compounds: $Zr_6Cl_{1.6}I_{10.4}Be$, $Zr_6Cl_{1.3}I_{10.7}B$, and $Zr_6Cl_{11.5}I_{1.5}B$. Matrix Effects and Halogen Substitution in Compact Network Structures

**Martin Köckerling, Ru-Yi Qi, and John D. Corbett***

Department of Chemistry, Iowa State University, Ames, Iowa 50011

*Received July 13, 1995*[⊗]

Investigations of the effect of halogen size on structure stability have been conducted in well-reduced and heavily interbridged zirconium chloride−iodide cluster systems. The title compounds are obtained in good yields from reactions of Zr, $ZrCl_4$, $ZrI_4$, and B or Be in sealed Ta tubes for ~4 weeks at 850 °C. Single-crystal diffraction at room temperature established these as $Zr_6Cl_{1.65(4)}I_{10.35(4)}Be$ and $Zr_6Cl_{1.27(3)}I_{10.73(3)}B$ [$R\bar{3}$, $Z = 3$, $a = 14.3508(8)$, 14.389(1) Å, $c = 9.8777(9)$, 9.915(2) Å, respectively] and $Zr_6Cl_{11.47(2)}I_{1.53(2)}B$ [$P4_2/mnm$, $Z = 2$, $a = 12.030(1)$ Å, $c = 7.4991(8)$ Å]. These are derivatives of the $Zr_6I_{12}C$ and orthorhombic $Zr_6Cl_{13}B$ structures, respectively, the latter containing unusual linear chains of clusters interbridged by $Cl^{i\text{-}i}$ that are in turn interconnected by three-bonded $Cl^{a\text{-}a\text{-}a}$ atoms. The random substitution of fractional Cl at specific I sites in the first two, and I for certain Cl in the third, was positionally resolved in all cases. The replacement always occurs at two-bonded $X^i$, so that single types of halogen are left in sites that interconnect clusters and generate the three-dimensional array. Structural changes seen in both structures are specifically related to relief of X···X crowding in the parent structure (matrix effects). Substitution of Cl for $I^i$ in the $Zr_6I_{12}C$ type greatly reduces intercluster I···I repulsions and allows, among other things, a 0.20 Å (5.8%) reduction in $Zr-I^{a\text{-}i}$ intercluster bond lengths. Increased Cl···I repulsions caused by I substitution in orthorhombic $Zr_6Cl_{13}B$ (*Pnnm*) convert the twisted chains and angular $Cl^{a\text{-}a\text{-}a}$ interchain bridges to planarity in tetragonal $Zr_6Cl_{11.5}I_{1.5}B$. Phase widths found are $0 \le x \le 1.4$ for $Zr_6Cl_xI_{12-x}Z$ (Z = B, Be) and $0 \le x \le 1.5$ for $Zr_6Cl_{13-x}I_xB$. The limit for iodine substitution in the chlorine-rich rhombohedral $Zr_6Cl_{12-x}I_xBe$ is about $x = 2.5$.

## Introduction

An astonishingly large variety of octahedral zirconium halide cluster compounds have been discovered in recent years. The key feature of these compounds is an interstitial atom in the center of every $Zr_6$ octahedron. Persistent efforts have so far revealed more than 30 distinct structure types.[1,2] The edges of the zirconium octahedra in all of these compounds are bridged by halogen, and halogen is also bound at the six metal vertices, these features giving rise to a family of compositions $A^{(I,II)}_x[(Zr_6X^i_{12}(Z)X^a_n]^3$ in which $A^{(I,II)}$ = a group 1 or 2 cation, $X^i$ = inner, edge-bridging halogen, $X^a$ = outer (exo) halogen, Z = interstitial, and $0 \le x, n \le 6$. The structure types depend first on the magnitude of *n* but usually also on *x* and, often, on the sizes of A, Z, and X as well.

The chlorides afford by far the largest variety of structures in which *n* ranges from 0 to 6, whereas iodide clusters have to date been found to adopt either the $Zr_6I_{12}Z$ (Z = C, B) ($n = 0$) structure[4,5] or a $Nb_6Cl_{14}$[6] type ($n = 2$) with the additional interstitial atom and, in some instances, alkali-metal cations.[1,2] Recent investigations of zirconium bromide systems have revealed, in addition to cluster phases with structure types already known, several connectivities and variations that have thus far been seen in neither chloride nor iodide systems.[7,8] This suggests that the size and basicity of the anions play important roles in the stability of specific cluster phases with respect to others. Therefore, a combination of two different halide ligands was considered a possible route to either new structure types or compounds with structural properties different from those with only one type of halide. The application of this concept to niobium systems has already been seen with the characterization of the $Nb_6Cl_{12-x}I_{2+x}$ ($x < 2$)[9] and $Nb_6I_{11-x}Br_x$ ($x < 2.7$),[10] these exhibiting a new halide bridging mode for the $M_6X_{14}$ stoichiometry and a rarely seen magnetic spin-crossover transition, respectively. The present paper focuses on the syntheses and structural characterizations of the first zirconium chloride iodide cluster compounds in the relatively well-reduced compounds $Zr_6Cl_{1.65}I_{10.35}Be$, $Zr_6Cl_{1.27}I_{10.73}B$, and $Zr_6Cl_{11.47}I_{1.53}B$ ($n = 0$, 1), each exhibiting some new and novel changes in a known structure type.

## Experimental Section

**Materials.** The preparation, handling, and purification of $ZrCl_4$ and $ZrI_4$ by repeated sublimation are described in refs 11 and 12. Finely powdered Zr metal was obtained by a process of hydrogenation, grinding, and subsequent dehydrogenation of reactor-grade crystal bar Zr sheets (<500 ppm of Hf). Amorphous boron (Aldrich, 99.999%, degassed at room temperature prior to use) and beryllium chunks (Aldrich, 99.9%) were the sources of the interstitials.

**Syntheses.** All compounds were handled only in a nitrogen-filled glovebox with moisture and oxygen levels less than 1 ppm (volume). Guinier powder patterns, obtained with the aid of Cu Kα radiation (λ

[⊗] Abstract published in *Advance ACS Abstracts,* February 15, 1996.

(1) Ziebarth, R. P.; Corbett, J. D. *Acc. Chem. Res.* **1989**, *22*, 256.
(2) (a) Corbett, J. D. In *Modern Perspectives in Inorganic Crystal Chemistry*; Parthé, E., Ed.; Kluwer Academic Publishers: Dordrecht, The Netherlands, 1992; p 27. (b) Corbett, J. D. *J. Alloys Compd.* **1995**, *229*, 10.
(3) Recent investigations reveal cluster examples with more complicated cation−anion combinations, e.g., $(Cs^+_3)(ZrCl_5)^-(Zr_6Cl_{15}Mn)^{2-}$: Zhang, J.; Corbett, J. D. *Inorg. Chem.* **1995**, *34*, 1652.
(4) Smith, J. D.; Corbett, J. D. *J. Am. Chem. Soc.* **1985**, *107*, 5704.
(5) Smith, J. D.; Corbett, J. D. *J. Am. Chem. Soc.* **1986**, *108*, 1927.
(6) Simon, A.; von Schnering, H.-G.; Wöhrle, H.; Schäfer, H. *Z. Anorg. Allg. Chem.* **1965**, *339*, 155.
(7) Qi, R.-Y.; Corbett, J. D. *Inorg. Chem.* **1995**, *34*, 1646.
(8) Qi, R.-Y. Ph.D. Dissertation, Iowa State University, 1993.
(9) Sägebarth, M.; Simon, A. *Z. Anorg. Allg. Chem.* **1990**, *587*, 119.
(10) Yoshiasa, A.; Borrmann, H.; Simon, A. *Z. Anorg. Allg. Chem.* **1994**, *620*, 1329.
(11) Daake, R. L.; Corbett, J. D. *Inorg. Synth.* **1983**, *22*, 26.
(12) Guthrie, D. H.; Corbett, J. D. *J. Solid State Chem.* **1981**, *37*, 256.

0020-1669/96/1335-1437$12.00/0 

**Table 1.** Selected Crystallographic Data for $Zr_6Cl_{1.65}I_{10.35}Be$, $Zr_6Cl_{1.27}I_{10.73}B$, and $Zr_6Cl_{11.47}I_{1.53}B$

| compn | $Zr_6Cl_{1.65(4)}I_{10.35(4)}Be$ | $Zr_6Cl_{1.27(3)}I_{10.73(3)}B$ | $Zr_6Cl_{11.47(2)}I_{1.53(2)}B$ |
|---|---|---|---|
| fw | 1928 | 1965 | 1159 |
| $d_{calc}$, g cm$^{-3}$ | 5.453 | 5.506 | 3.547 |
| space group, $Z$ | $R\bar{3}$ (No. 148), 3 | $R\bar{3}$ (No. 148), 3 | $P4_2/mnm$ (No. 136), 2 |
| $a$, Å[a] | 14.3508(8) | 14.389(1) | 12.030(1) |
| $c$ Å | 9.8777(9) | 9.915(2) | 7.4991(8) |
| $V$, Å$^3$ | 1761.7(3) | 1777.8(5) | 1085.3(2) |
| abs coeff $\mu$(Mo K$\alpha$), cm$^{-1}$ | 163.4 | 166.4 | 63.5 |
| $R$,[b] % | 4.19 | 3.20 | 3.15 |
| $R_w$,[b] % | 4.17 | 3.01 | 2.50 |

[a] From Guinier data with internal Si standard; $\lambda$ = 1.540 562 Å; 21 °C. [b] $R = \sum||F_o| - |F_c||/\sum|F_o|$, $R_w = [\sum w(|F_o| - |F_c|)^2/\sum w|F_o|^2]^{1/2}$, $w = (1/\sigma_F^2)^{1/2}$.

= 1.540 562 Å) on an Enraf-Nonius camera, were used to identify phases in the reaction products by comparison of their patterns with those calculated on the basis of single-crystal data for prototype structures. Phase yields were estimated visually according to the relative intensity distributions on the Guinier films. Precise lattice parameters of new phases with known structures were obtained from these patterns as well by least-squares refinements of the positions of indexed reflections using lines from added NIST Si as an internal standard.

A phase near $Zr_6Cl_{1.65}I_{10.35}Be$ was first seen along with lines of a second phase in the product of a reaction loaded with the stoichiometry $Zr_6Cl_4I_8Be$ and carried out at 850 °C for 28 days. The other phase, not further reported here, was repeatedly seen in many reactions run in the mixed iodide/chloride systems, not only with Be as the interstitial but also with B.[13] A later reaction loaded at the stoichiometry obtained from the structural refinement of the former $Zr_6X_{12}Be$ phase gave it in >90% yield. Further reactions were also run with different I/Cl ratios to explore the phase width of this mixed-halide cluster.

The synthetic procedure leading to the chlorine-rich $Zr_6Cl_{11.47}I_{1.53}B$ was similar. It was first seen in the Guinier pattern of the product from a reaction loaded as $Zr_6Cl_7IB$, and held at 820 °C for 40 days, while later reactions run according to the structurally refined stoichiometry gave this phase in >90% yield. Again, a series of reactions was run over the composition range $Zr_6Cl_3I_{10}B$ to $Zr_6Cl_{10}I_3B$ to examine the phase breadth. Crystals of the second rhombohedral phase studied, $Zr_6Cl_{1.27}I_{10.73}B$, were also isolated from the product of the iodide-richest reaction and beyond. This phase is again obtained in high yield whenever a reaction is run close to the refined stoichiometry.

None of the above products could be obtained in the absence of B or Be.

**Crystal Structure Studies. $Zr_6Cl_{1.65(4)}I_{10.35(4)}Be$.** The powder pattern line distribution for the first reaction product above suggested a compound with the rhombohedral $Zr_6I_{12}Z$[4,5] structure type, but the shift of lines to higher angles indicated probable incorporation of chloride into the iodide structure. The positions of the lines indexed with a hexagonal lattice refined to give cell parameters $a$ = 14.3508(8) Å, $c$ = 9.8777(9) Å, $V$ = 1761.7(3) Å$^3$, which are significantly smaller than those for $Zr_6I_{12}B$ ($a$ = 14.534(1) Å, $c$ = 9.986(1) Å, $V$ = 1825(1) Å$^3$ [5]) even though the Be interstitial is larger.[1,2] Black hexagonal crystals were sealed in capillaries by flame, and the diffraction data were collected from one at room temperature on an Enraf-Nonius CAD4 diffractometer in order to determine the anion distribution. The initial cell from 25 randomly located and centered orientation reflections properly transformed to the correct rhombohedral cell in the hexagonal setting. Two octants of data up to 50° in 2$\theta$ were collected without restrictions, and space group $R\bar{3}$ (No. 148) was chosen on the basis of the systematic extinctions, the intensity statistics, and the earlier structure determinations for $Zr_6I_{12}Z$.[4,5] This was later shown to be correct by comparison of the refinement results with those obtained in $R3$ (No. 146). The data reduction involved Lorentz and polarization corrections as well as an empirical absorption correction with the average of three $\psi$-scans.[14] Averaging in Laue group $\bar{3}$ resulted in $R_{ave}$ = 3.4% for the observed data ($I > 3\sigma_I$).

The atom positions of $Zr_6I_{12}C$ were utilized as the initial model, and these refined well.[15] The isotropic thermal parameter of I2 turned out to be significantly larger than that of I1, indicating partial occupancy of the former site by chlorine was probable. After refinement of the site occupancy as iodine, a difference Fourier map showed a separate, close, and smaller peak that was suitably disposed about 2.5 Å from the two neighboring zirconium atoms to be an inner bridging Cl atom. This was so refined isotropically with the sum of the occupancies of Cl and I2 constrained to unity. At this stage, refinement of the I1 occupancy gave a value close to unity, at which it was subsequently kept fixed. Anisotropic refinement of the Zr and I atoms and isotropic refinement of the Be and the Cl atoms converged at $R(F)$ = 4.2%, $R_w$ = 4.2%. Final refinement of the occupancies of the I2/Cl sites gave the empirical formula $Zr_6Cl_{1.65(4)}I_{10.35(4)}Be$. The largest peaks in the final difference Fourier map were +2.17 e/Å$^3$, 0.42 Å from Zr, and −1.53 e/Å$^3$. Some data collection and structure refinement parameters are compiled in Table 1.

**$Zr_6Cl_{1.27(3)}I_{10.73(3)}B$.** This compound, with the same general $Zr_6X_{12}Z$-type pattern as above, was found in the products of the iodine-richest $Zr_6X_{12}B$ reaction. Diffraction data were collected at room temperature from a black crystal over two octants ($2\theta_{max}$ = 50°) on the same diffractometer, and the structure refinement proceeded in a manner similar to that just described after an absorption correction with the average of six $\psi$-scans. The I2 position could again be split into two, and anisotropic refinement of the Zr and I atoms with isotropic variation of Cl and B gave final values of $R$ = 3.2%, $R_w$= 3.0%, the composition $Zr_6Cl_{1.27(3)}I_{10.73(3)}B$, and the largest $\Delta F$ residual of 1.6 e/Å$^3$.

**$Zr_6Cl_{11.47}I_{1.53}B$.** The Guinier powder pattern of what turned out to be this compound looked similar to that calculated for orthorhombic $Zr_6Cl_{13}B$,[16,17] suggesting a closely related structure with somewhat larger dimensions. One octant of diffraction data ($2\theta$ < 50°) from a black single crystal was collected on a Rigaku AFC6R diffractometer at room temperature. Subsequently, all the lines from the Guinier pattern could be indexed in the same primitive tetragonal lattice with $a$ = 12.030(1) Å, $c$ = 7.4991(8) Å, $V$ = 1085.3(2) Å$^3$. The data were reduced and corrected as before with the aid of the average of three $\psi$-scans, which yielded $R_{ave}$ = 2.9% for the observed data ($3\sigma_I$ cutoff) in Laue group $4/mmm$. The systematic absences ($k + l \neq 2n$ for $0kl$) are consistent with space groups $P4_2/mnm$ (No. 136), $P\bar{4}n2$ (No. 118), and $P4_2nm$ (No. 102). The first was chosen on the basis of intensity statistics and was later verified by the successful refinement of the structural model.

All the Zr and Cl atoms in the asymmetric unit were located by direct methods included in the SHELX-86 program.[18] The interstitial B was added to the structure model on the basis of the synthetic procedure as well as common knowledge of these cluster halide phases. The Cl1, Cl2, and Cl3 atoms had reasonable thermal parameters after isotropic refinement, whereas that for Cl4 appeared rather small. What was presumed to be a fractional iodine atom was found close to Cl4 in a difference Fourier map and was included in the model. High

(13) Preliminary structural results indicate that this phase contains Zr octahedra condensed in one lattice direction and fewer than 12 halides per octahedron: Köckerling, M.; Qi, R.-Y.; Corbett, J. D. Unpublished.

(14) Data reduction was performed with the following program package: TEXSAN, version 6.0; Molecular Structure Corp.: The Woodlands, TX, 1990.

(15) Least-squares refinements were done with the following program package: *SHELXTL-PLUS*; Siemens Analytical X-ray Instruments Inc.: Madison, WI, 1990.

(16) Ziebarth, R. P.; Corbett, J. D. *J. Am. Chem. Soc.* **1985**, *107*, 4571.
(17) Ziebarth, R. P. Ph.D. Dissertation, Iowa State University, 1987.
(18) Sheldrick, G. M. SHELX-86. Universität Göttingen, Germany, 1986.

**Table 2.** Positional and Isotropic Displacement Parameters (Å²) for $Zr_6Cl_{1.65}I_{10.35}Be$, $Zr_6Cl_{1.27}I_{10.73}B$, and $Zr_6Cl_{11.47}I_{1.53}B$

| atom | position | *x* | *y* | *z* | $U_{eq}$[a] |
|---|---|---|---|---|---|
| | | $Zr_6Cl_{1.65(4)}I_{10.35(4)}Be$ | | | |
| Zr | 18f | 0.15072(9) | 0.0425(1) | 0.1410(1) | 1.17(5) |
| I1 | 18f | 0.35249(7) | 0.1011(1) | 0.33391(9) | 2.56(5) |
| I2[b] | 18f | 0.1277(2) | 0.1787(3) | 0.3307(3) | 2.49(8) |
| Cl[b] | 18f | 0.119(2) | 0.165(3) | 0.295(2) | 3.0(8) |
| Be | 3a | 0 | 0 | 0 | 0.01(62) |
| | | $Zr_6Cl_{1.27(3)}I_{10.73(3)}B$ | | | |
| Zr | 18f | 0.14682(6) | 0.04163(8) | 0.13586(7) | 0.91(3) |
| I1 | 18f | 0.35212(4) | 0.10132(6) | 0.33331(5) | 2.05(3) |
| I2[c] | 18f | 0.1271(1) | 0.1783(1) | 0.3288(2) | 1.87(5) |
| Cl[c] | 18f | 0.119(2) | 0.166(3) | 0.294(2) | 2.7(6) |
| B | 3a | 0 | 0 | 0 | 0.01(35) |
| | | $Zr_6Cl_{11.47(2)}I_{1.53(2)}B$ | | | |
| Zr1 | 8j | 0.40255(6) | *x* | 0.2145(1) | 1.78(2) |
| Zr2 | 4g | 0.63600(9) | -*x* | 0 | 1.83(4) |
| Cl1 | 2a | 0 | 0 | 0 | 2.5(1) |
| Cl2 | 4g | 0.2009(2) | -*x* | 0 | 2.3(1) |
| Cl3 | 4j | 0.2904(2) | *x* | 0 | 2.6(1) |
| Cl4[d] | 16k | 0.545(1) | 0.2467(7) | 0.242(2) | 2.9(2) |
| I[d] | 16k | 0.538(1) | 0.2125(8) | 0.254(2) | 2.7(2) |
| B | 2b | 0 | 0 | 0.5 | 2.3(7) |

[a] $\times 10^2$. The isotropic-equivalent temperature factor $U_{eq}$ is defined as one-third of the trace of the orthogonalized $\mathbf{U}_{ij}$ tensor: $U_{eq} = {}^1/_3 \sum_{i=1}^{3}\sum_{j=1}^{3} a_i^* a_j^* U_{ij} \vec{a}_i \vec{a}_j$. [b] Split position: I2, 72.6(7)%; Cl, 27.4(7)%. [c] Split position: I2, 78.8(4)%; Cl, 21.2(4)%. [d] Split position: I, 19.1(2)%; Cl4, 80.9(2)%.

correlation coefficients made a step-by-step refinement of the occupancies and thermal parameters necessary. The isotropic temperature factors for both Cl4 and I were at first fixed at $B = 2.0$ Å², and the occupancies and positions of both atoms were refined while the former were constrained to a sum of unity. In the next stage, the refined occupancies were held fixed, and the thermal parameters were refined independently. This procedure was repeated several times until the parameters did not change any more. During this procedure, the *R* value slowly dropped by about 4%. Finally, anisotropic refinement of all atoms but B and with the sum of the occupancies of Cl4 and I constrained to unity converged at $R = 3.2\%$, $R_w = 2.5\%$. The largest positive and negative peaks in the final difference Fourier map were 0.94 and −0.89 e/Å³. The empirical formula from this refinement is $Zr_6Cl_{11.47(2)}I_{1.53(2)}B$. The small $U_{eq}$ values for interstitial B or Be in all three structures are fairly characteristic of light atoms centering clusters.

The additional information in the Supporting Information as well as $F_o/F_c$ data are available from J.D.C.

## Results and Discussion

Exploratory reactions were conducted in zirconium cluster systems with mixed chloride and iodide anions in order to locate new structural examples in which both participated in the edge- and intercluster-bridging functions. The results support the distinctions already known between pure chloride and iodide systems of zirconium (cf. Introduction) and illustrate particularly well those size-dependent structural properties known under the rubric "matrix effects".[19] The syntheses and structures of the first three mixed chloride−iodide compounds have now been established for $Zr_6Cl_{1.65}I_{10.35}Be$, $Zr_6Cl_{1.27}I_{10.73}B$, and $Zr_6Cl_{11.47}I_{1.53}B$. The atom coordinates and isotropic-equivalent displacement parameters for these are given in Table 2. Important bond distances calculated with the more accurate cell dimensions refined from Guinier powder diffraction analyses are listed in Table 3.

**Rhombohedral Phases.** The isostructural $Zr_6Cl_{1.65}I_{10.35}Be$ and $Zr_6Cl_{1.27}I_{10.73}B$ adopt the $R\bar{3}$ structure of $Zr_6I_{12}Z$ (Z = C, B),[4,5] a structure that is also known for $Zr_6Br_{12}Z$ (Z = H, Be, B)[8,20] and $Zr_6Cl_{12}Z$ (Z = H, Be).[20] As with all zirconium halide cluster phases, the principal building blocks are $Zr_6X_{12}(Z)$ clusters in which the nominal octahedral $Zr_6(Z)$ cores have all 12 edges bridged by halide atoms ($X^i$). All six metal vertices are further bonded via exo halide functions ($X^a$), as shown in Figure 1 for the berylide cluster in which both I2 and the Cl positions that substitute for I2 are plotted ($\bar{3}$ axis vertical). The [110] section in Figure 2 illustrates how the clusters in $Zr_6(Cl,I)_{12}Z$ phases define an interbridged, cubic-close-packed array, with vertical $\bar{3}$ axes through Z. From another point of view, Figure 2 can be described as *ccp* layers of halogen (with interstitial Be or B regularly substituted therein) that lie normal to the crystallographic *c* direction, and between which groups of octahedral holes are filled by Zr atoms in an ordered way such that a similar array of $Zr_6X_{12}Z$ clusters is formed.

The interconnectivities of the clusters and, thereby, the different functionalities of the halogen atoms can be systematically described as $[Zr_6(I,Cl)^i{}_6I^{i\text{-}a}{}_{6/2}I^{a\text{-}i}{}_{6/2}Z]$ if the atoms in bridging (i-a, a-i) functions are divided equally. The six I1 atoms that bridge edges around the waist of each $Zr_6(Z)$ octahedron in this view generate the three-dimensional cluster arrangement inasmuch as they are further bonded, alternately up and down, to exo positions on adjacent clusters to give them $I^{i\text{-}a}$ and $I^{a\text{-}i}$ functions. In fact, an important building principle revealed by the present work is that the three-dimensional structure arrangements are seemingly always achieved with only one type of halide. Mixed halides in the positions that provide these connections would likely require a much larger cell (ordered superstructure), a lower symmetry, or, less likely in such a tightly packed structure, complete disorder. Instead, the six I2 atoms that are two-bonded to a single $Zr_6(Z)$ trigonal antiprism, above and below each cluster in this view, are randomly occupied by 27.5(7)% chlorine and 72.5(7)% iodine in the beryllide and 21.2(4)% Cl and 78.8(4)% I in the boride, but in resolvable split positions.

**Matrix Effects.** The distinctive and meaningful changes that occur on substitution of some chloride into these iodide clusters can be understood in terms of "matrix effects", in these cases inter- and intracluster distances and angles that are influenced or largely determined by I···I (vs I···Cl) contacts.[19] A well-known example is the variation in $d(Zr-I^{a\text{-}i})$ distances in $Zr_6I_{14}Z$ phases in which the $I^a$ positions are fixed largely by $I^a\cdots I^i$ contacts but the metal vertices move in response to the size of Z.[21] The particularly pertinent volume, distance, and angle data for the two mixed halides reported here, along with the same measures for $Zr_6I_{12}Z$ (Z = C, B), are collected in Table 4. (The unlisted parameters *c*/*a*, $\bar{d}(Zr-I2^i)$, $\bar{d}(Zr-I1^{i\text{-}a})$ vary only by small amounts.) The cluster sizes reflected in $d(Zr-Z)$ and $\bar{d}(Zr-Zr)$ are determined mainly by the effective sizes of Z: C < B < Be.[1,2] The skeletal electron counts in the clusters listed in Table 4 are 16, 15, 15, 14 e, respectively; however, these afford at best second-order effects. The $a_{2u}$ HOMO in the first three is mainly Zr−Zr bonding, with contributing $Zr-I^i$ $\pi^*$ effects reduced by matrix effects of intracluster closed-shell $I^i\cdots I^i$ repulsions (3.98−4.07 Å), which cause the Zr vertices to lie appreciably inside the $I^i$ cube.[22] (This characteristic is seen best at the lower left vertices of the clusters in Figure 2; the trans I1−Zr−I2 angles are given in Table 4.) Other closed-shell I···I interactions in such a tightly bound network have readily discernible effects. Experience has shown that $d(I\cdots I) \leq 4.00$ Å are pretty tight when both are bound to zirconium. Hence,

(19) Corbett, J. D. *J. Solid State Chem.* **1981**, *37*, 335.
(20) Ziebarth, R. P.; Corbett, J. D. *J. Solid State Chem.* **1989**, *80*, 56.
(21) Hughbanks, T.; Rosenthal, G.; Corbett, J. D. *Inorg. Chem.* **1988**, *110*, 1511.
(22) Ziebarth, R. P.; Corbett, J. D. *J. Am. Chem. Soc.* **1989**, *111*, 3272.

**Table 3.** Important Bond Distances (Å) for $Zr_6Cl_{1.65}I_{10.35}Be$, $Zr_6Cl_{1.27}I_{10.73}B$, and $Zr_6Cl_{11.47}I_{1.53}B$

| | $Zr_6Cl_{1.65}I_{10.35}Be$ | | $Zr_6Cl_{1.27}I_{10.73}B$ | | $Zr_6Cl_{11.47}I_{1.53}B$ | | |
|---|---|---|---|---|---|---|---|
| Zr−Zr | | | | | | | |
| intralayer[a] | 3.345(2) | ×6[b] | 3.266(1) | ×6 | Zr1−Zr1 | 3.316(2) | ×2 |
| interlayer | 3.391(2) | ×6 | 3.289(1) | ×6 | | 3.217(2) | ×2 |
| $\bar{d}$ | 3.368 | | 3.278 | | Zr1−Zr2 | 3.269(1) | ×8 |
| | | | | | $\bar{d}$ | 3.268 | |
| $Zr-I2^i$ | 2.834(3) | ×6 | 2.847(2) | ×6 | $Zr1-I^i$ | 2.828(11) | ×8 |
| | 2.844(3) | ×6 | 2.858(2) | ×6 | $Zr2-I^i$ | 2.887(13) | ×8 |
| $\bar{d}$ | 2.853 | | 2.853 | | $\bar{d}$ | 2.858 | |
| $Zr-Cl^i$ | 2.54(3) | ×6 | 2.56(2) | ×6 | $Zr1-Cl3^i$ | 2.496(3) | ×4 |
| | 2.54(2) | ×6 | 2.55(2) | ×6 | $Zr1-Cl4^i$ | 2.549(10) | ×8 |
| $\bar{d}$ | 2.54 | | 2.56 | | $Zr2-Cl4^i$ | 2.544(12) | ×8 |
| | | | | | $\bar{d}$ | 2.536 | |
| $Zr-I1^{i-a}$ | 2.929(1) | ×6 | 2.940(1) | ×6 | $Zr1-Cl1^{i-i}$ | 2.708(1) | ×4 |
| | 2.913(2) | ×6 | 2.917(1) | ×6 | | | |
| $\bar{d}$ | 2.921 | | 2.929 | | | | |
| $Zr-I1^{a-i}$ | 3.207(1) | ×6 | 3.289(1) | ×6 | $Zr1-Cl2^{a-a-a}$ | 2.772(1) | ×4 |
| | | | | | $Zr2-Cl2^{a-a-a}$ | 2.774(1) | ×2 |
| Zr−interstitial | 2.382(1) | ×6 | 2.318(1) | ×6 | Zr1−B | 2.310(1) | ×4 |
| | | | | | Zr2−B | 2.314(1) | ×2 |
| | | | | | $\bar{d}$ | 2.311 | |
| | | | | | I−Cl2 | 3.574[c] | |
| | | | | | | 3.616[c] | |
| | | | | | I−Cl3 | 3.532[d] | |
| | | | | | | 3.623[c] | |

[a] Layers normal to *c*. [b] Number of times the distance occurs per cluster. [c] Intrachain distance. [d] Interchain distance.

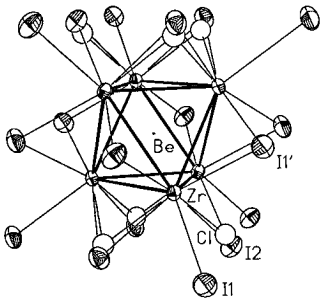


**Figure 1.** View of the $[Zr_6(Cl,I)^i{}_6I^{i-a}{}_6I^{a-i}{}_6]$ cluster in $Zr_6Cl_{1.65}I_{10.35}Be$ (70% probability thermal ellipsoids). Zr−Zr bonds are emphasized, and the chlorine atoms are drawn with open ellipsoids.

Table 4 lists only the shorter I···I distances, excluding larger intracluster I1···I1 (around the cluster waist, normal to $\vec{c}$) and I1···I2 contacts as well as intercluster types for I1···I2 (between layers) and I2···I2 (approximately parallel to $\vec{c}$). The pertinent data remaining in Table 4 show some significant variations, particularly evident when Cl substitutes for I2 with a fixed boron interstitial, as follows:

(1) The change in cell volume between $Zr_6I_{12}C$ and $Zr_6I_{12}B$ is very slight, not an increase originating with the size of Z, doubtlessly because an expansion from a matrix effect is already present in the carbide, but these are followed by a 47(1) Å$^3$ (2.6%) decrease when chloride is substituted for some $I2^i$ in the boride and another 16 Å$^3$ decrease when (more) chloride is incorporated, even with a larger Be interstitial. (More nearly normal B → Be effects in the last step with fixed halide can be approximated as the +19.5(3) Å$^3$ change in cell volume seen in the corresponding $Zr_6Br_{12}Z$,[8,20] and a $\Delta d$(Zr−Z) of +0.027 Å for this change in variety of chlorides.[1,2])

(2) Meaningful changes in cluster proportions are found in both *d*(Zr−Zr) intralayer (within the basal faces of the antiprism, Δ) and interlayer (Δ-∇, between). The $\bar{d}$(Zr−Zr) distances both increase, as expected for the C−B−Be conversions, but faster along *z* so the *d*(Zr−Zr) differences change from a 0.010(1) Å axial compression with C to a 0.046(3) Å elongation with Be.

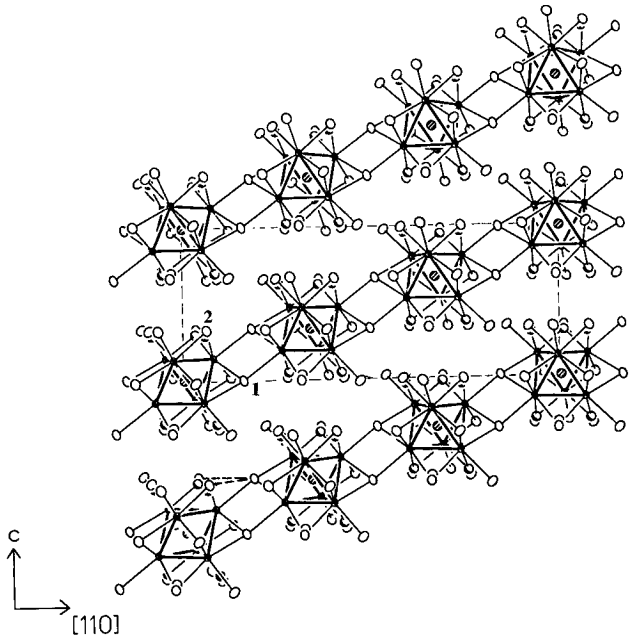


**Figure 2.** [110] section of the rhombohedral structure of $Zr_6Cl_{1.65}I_{10.35}$-Be and $Zr_6Cl_{1.27}I_{10.73}B$ ($\vec{c}$ vertical). The iodine atoms are drawn with open ellipsoids, and chlorines are shaded. Two (of six) of the $Zr-I^{i-a}$, $Zr-I^{a-i}$ pairs of intercluster bridges (rhomboids) per cluster are illustrated. Close-packed layers of halogen (and interstitials) run horizontally. A pair of the short I1···I2 intercluster contacts are marked at the lower left.

The effect of chloride substitution in the boride is mainly a 0.025 Å shrinkage in the basal edge.

(3) The striking decreases in cell volume that occur on substitution of chloride for ∼25% of the two-bonded axial iodide ($I2^i$) atoms can be tied to the relief of substantial matrix effects (repulsions) in the two ternary iodides. These can be recognized and followed particularly in the *inter*cluster distances highlighted by bold type in Table 4, namely, by the nearly 0.2 Å decrease in intercluster bridge lengths $d(Zr-I1^{a-i})$, six about each cluster, and the 0.07 Å reduction in *d*(I1···I2) between atoms in the

**Table 4.** Significant Changes in Volume (Å$^3$), Distances (Å), and Angles (deg) in Four Iodine-Rich $Zr_6X_{12}Z$ Phases ($R\bar{3}$)

| | $Zr_6I_{12}C$[a] | $Zr_6I_{12}B$[b] | $Zr_6I_{10.7}Cl_{1.3}B$ | $Zr_6I_{10.4}Cl_{1.6}Be$ |
|---|---|---|---|---|
| cell vol | **1824** | **1825** | **1778** | **1762** |
| $d$(Zr−Z) | 2.259(1) | 2.327(1) | 2.318(1) | 2.382(1) |
| $d$(Zr−Zr) | | | | |
| intra Δ | 3.200(1) | 3.291(1) | 3.266(1) | 3.345(2) |
| inter Δ-∇ | 3.190(1) | 3.292(2) | 3.289(1) | 3.391(2) |
| diff | 0.010 | ∼0 | −0.023 | −0.046 |
| $\bar{d}$ | 3.195 | 3.292 | 3.278 | 3.368 |
| $\bar{d}$(Zr−I$^{a\text{-}i}$) | **3.403(1)** | **3.344(2)** | **3.289(1)** | **3.207(1)** |
| $\bar{d}$(I···I) | | | | |
| I2···I2 (intracluster) | 3.980(1) | 4.001(1) | 3.963(3) | 3.964(4) |
| I1···I1 (inter, across rhomboid) | 4.008(1) | 3.994(1) | 3.979(1) | 3.974(2) |
| I1···I2 (inter, normal to $\vec{c}$) | 3.979(1) | **3.978(2)** | **3.922(2)** | **3.905(2)** |
| | 3.980(1) | **3.987(1)** | **3.923(1)** | **3.910(3)** |
| trans ∠I1−Zr−I2 | 157.5(1) | 159.7(1) | 158.6(1) | 161.2(1) |
| %Cl in X2 posn | 0 | 0 | 21.2(4) | 27.5(7) |

[a] Reference 4. [b] Reference 5.

same puckered halogen layer but in different clusters, 12 per cluster. The increased Zr−I$^{a\text{-}i}$ bonding attained must be much of the driving force for chlorine substitution. The shortest $d$(I···I) in $Zr_6I_{12}C$, and presumably the principal volume-limiting interaction, are the lateral I1···I2 contacts within halogen layers and between clusters[23] plus the intracluster I2···I2 separations, each with two per atom. (A pair of the former are marked at the lower left of Figure 2.) Random substitution of ∼25% of the I2 by the smaller and more closely bonded chloride allows formal decreases in the two types of intercluster I···I contacts of ∼0.07 and ∼0.02 Å (and ∼0.03 Å in intracluster $d$(I2···I2)) over the series, even with the change to the larger Be. Of course, these really represent the effect of ∼25% random I2 vacancies. The increase in the relative height of the $Zr_6$ antiprism in response to stronger Zr−I$^{a\text{-}i}$ bonding also keeps the next shorter I1···I1 separations across the rhomboids (where there is no substitution) from decreasing to less than 3.97 Å. The I2···I2 gap between clusters along $\vec{c}$ remains ≥4.05 Å. (Dimensional problems around the 0, 0, 0.5 site therein that is occupied by the seventh metal atom in $Sc(Sc_6I_{12}C)$[24] and so forth[25] may be involved in the limited successes at substitution chemistry at the added metal site.[26]) The relatively unperturbed Zr−Cl$^i$ distances in all three structures, 2.50−2.56 Å, correspond closely to those in many $Zr_6Cl^i_{12}$-type situations.

Assuming that only iodine atoms are used for cluster interconnections, the theoretical phase breadth of the rhombohedral structure would be from $Zr_6I_{12}Z$ to $Zr_6Cl_6I_6Z$, or $Zr_6(I_xCl_{6-x})^iI_6Be$ with $0 \le x \le 6$ if we include the end stoichiometries. The intrusion of yet another phase limits the actual chlorine range substantially (below).

**Tetragonal $Zr_6X_{13}B$.** The structure of $Zr_6Cl_{11.47}I_{1.53}B$ is very closely related to that of the novel orthorhombic $Zr_6Cl_{13}B$, which has been briefly mentioned in the literature[2,16] but not thoroughly described or discussed.[17] The structural framework of $Zr_6Cl_{13}B$ (assigned on the basis of powder patterns) and $KZr_6Cl_{13}Be$ (refined in space group *Pnnm* from single-crystal data) exhibits two modes of intercluster connectivity that are unique in the family of zirconium cluster halides. One consists of linear chains of $Zr_6Cl_{12}B$-type clusters along $\vec{c}$ (Figure 3) interconnected via shared coplanar Cl1$^{i\text{-}i}$ atoms that are four-bonded to Zr1, viz., $Zr_6(B)Cl^i_{10}Cl^{i\text{-}i}_{2/2}$. (More examples of this connectivity are found among rare-earth-metal iodides, either with isolated clusters, for instance in the recently reported $Pr_{12}I_{17}Fe_2$,[27] or between condensed cluster chains.[25]) The second unique feature is two Cl2$^{a\text{-}a\text{-}a}$ atoms per cluster that bond exo to three metal vertices and interconnect the linear chains into a three-dimensional network, viz., $Zr_6(B)Cl^i_{10}Cl^{i\text{-}i}_{2/2}Cl^{a\text{-}a\text{-}a}_{6/3}$. The two modes are illustrated in Figure 3 with all Cl$^i$ omitted. The apex Zr2, Cl1$^{i\text{-}i}$, and Cl2$^{a\text{-}a\text{-}a}$ all lie on basal mirror planes of the cell ($z = 0, 1$). The tribridges are slightly nonplanar, as evident in the [001] projection along chains of the chloride beryllide in Figure 4, which shows the pseudo-body-centered arrangement with adjoining chains translated by $\vec{c}/2$. Close-packed chlorine (plus Be) layers sequenced $(ch)_2$ are evident normal to $\vec{a}$ as well. In $KZr_6Cl_{13}Be$, every other cavity in each channel along $\vec{c}$ (i.e., the cell edges $^1/_2$, 0, 0, etc.) is filled with potassium. These 10-coordinate sites are large enough, and the network sufficiently flexible, to encrypt a major fraction with rubidium cations through ion exchange with liquid $RbAlCl_4$ at 350 °C.[17]

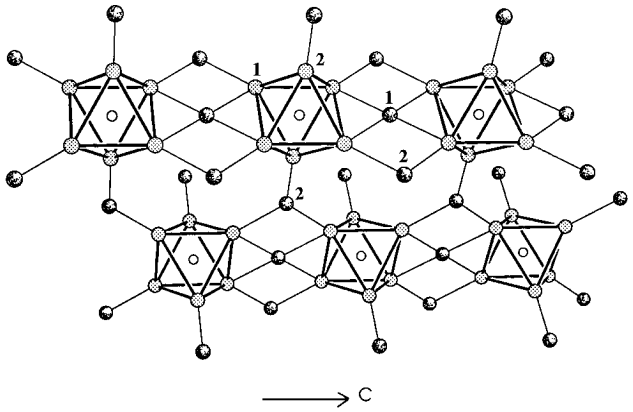


**Figure 3.** Schematic representation of the intercluster connectivity in the $Zr_6Cl_{13}B$ structure. Edge-bridging chlorines are omitted for clarity. Intercluster bridging chlorines are irregularly shaded, Zr atoms are regularly dotted, and interstitial atoms are open circles. The Cl1$^{i\text{-}i}$ atoms trans-bridge clusters into chains along $\vec{c}$ while Cl2$^{a\text{-}a\text{-}a}$ atoms bound exo at all cluster vertices interconnect the chains. (Some of the latter functions are not all shown in the drawing.)

A drawing of a single $Zr_6(Z)$ octahedra and all of surrounding halides in the $Zr_6Cl_{11.47}I_{1.53}B$ version is given in Figure 5 with 70% probability displacement ellipsoids. The trans bridging of the $Zr_6(Z)$ clusters via the interchain Cl1$^{i\text{-}i}$ atoms yields a

(23) A third longer intercluster I1···I2 contact about each atom type occurs in the same halogen layer and ranges between 4.066 and 3.995 Å over the series in Table 4. This lies about normal to the rhomboid connections seen in Figure 2 and involves I2 in a cluster in the third layer.

(24) Dudis, D. S.; Corbett, J. D.; Hwu, S.-J. *Inorg. Chem*. **1986**, *25*, 3434.
(25) Simon, A.; Mattausch, Hj.; Miller, G. J.; Bauhofer, W.; Kremer, R. K. In *Handbook on the Physics and Chemistry of Rare Earths;* Gschneider, K. A., Jr., Eyring, L., Eds.; North Holland: Amsterdam, 1991; Vol. 15, p 191.
(26) Hughbanks, T.; Corbett, J. D. *Inorg. Chem.* **1988**, *27*, 2022.
(27) Park, Y.; Corbett, J. D. *Inorg. Chem.* **1994**, *33*, 1705.

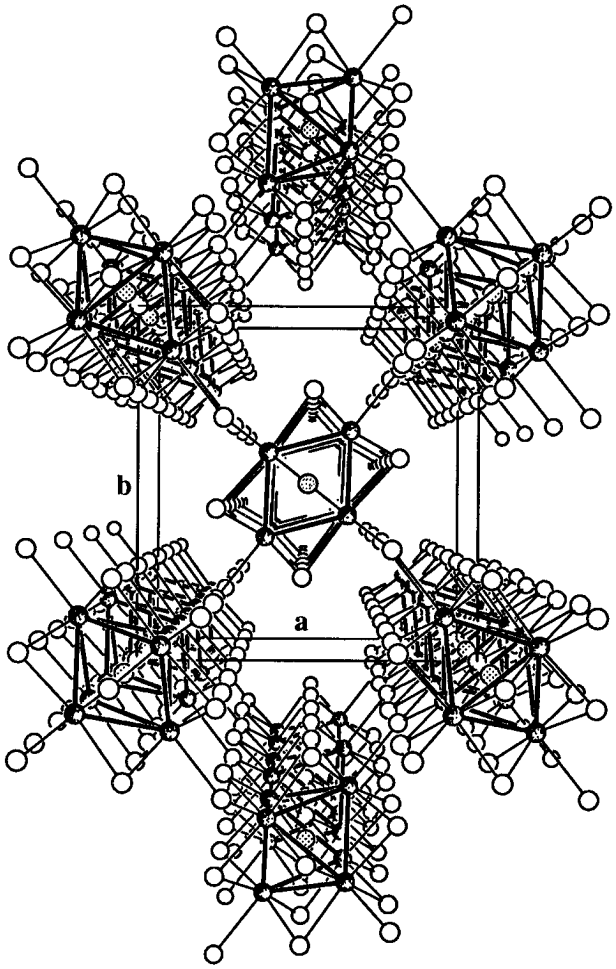


**Figure 4.** [001] view of the network structure in $KZr_6Cl_{13}Be$ and $Zr_6Cl_{13}B$. The channels between cluster chains, normal to the plane of the figure, are partially occupied by cations in the former phase. Zr atoms are randomly and the interstitial atoms regularly dotted, while chlorine atoms are open circles. The $Cl2^{a\text{-}a\text{-}a}$ atoms that interconnect chains alternate in projection with $Cl3^{i}$ atoms that bridge side edges of the clusters along the chains.

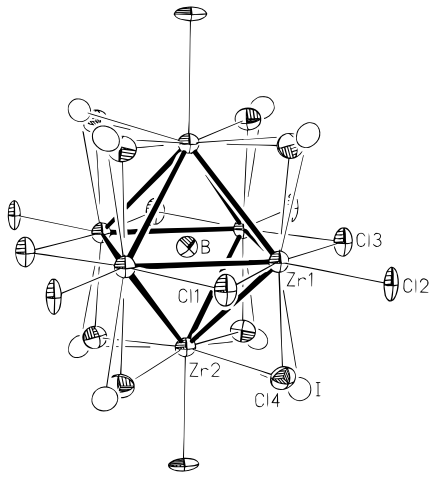


**Figure 5.** A single $Zr_6(Cl4,I)^{i}_8(Cl3^{i})_2(Cl1^{i\text{-}i})(Cl^{a\text{-}a\text{-}a})_{6/3}$ cluster in $Zr_6Cl_{11.47}I_{1.53}B$ (70% probability). The 19% iodine atoms that substitute for Cl4 are drawn as open ellipsoids.

rectangular $(Zr1)_4$ waist for the octahedron, 3.316(2) Å for the edge bridged by $Cl^{i\text{-}i}$ and 0.10 Å less for the side edge bridged by Cl3, while the Zr1−Zr2 distances to the apices are effectively the average (Table 3). The three trans Zr−Zr distances remain within $3\sigma$ of 4.623 Å. The average Zr−B distance, 2.311 Å, compares well with 2.303 Å in $Zr_6Cl_{14}B$,[20] where halide matrix effects are small, and the $\bar{d}$(Zr−Zr) value compares likewise, for geometric reasons. The shortest Zr−Zr distance between clusters is 4.282 Å within the chain. The Zr−Cl distances increase in the following order: $Cl3^{i}$ (on the short Zr1−Zr1 edge) at 2.496 Å, $Cl4^{i}$ at 2.547 Å (the rest of $Cl^{i}$), four-bonded $Cl1^{i\text{-}i}$, 2.708 Å, and three-bonded $Cl2^{a\text{-}a\text{-}a}$, 2.773 Å. (Exo bonds even of the $X^{a\text{-}a}$ type are characteristically longer.[2]) In $KZr_6Cl_{13}Be$, these various Zr−Cl distances are about 0.02 Å larger to all $Cl^{i}$ that have K neighbors, 0.010 Å less for $Cl^{i\text{-}i}$ with the larger Z, and 0.047 Å less at $Cl^{a\text{-}a\text{-}a}$ without iodine substitution. As in $KZr_6Cl_{13}Be$, only the exo B−Zr1(apex)−$Cl2^{a\text{-}a\text{-}a}$ direction in the present structure deviates from linearity, by ∼6.4°.

A novel and important role of iodine substitution in $Zr_6Cl_{11.5}I_{15}B$ is to increase the space group symmetry from orthorhombic *Pnnm* for $Zr_6Cl_{13}B$ to the tetragonal supergroup $P4_2/mnm$. Symmetrywise, this includes the addition of [110] and [1$\bar{1}$0] mirror planes to Figure 4. This changes the angle between the apical Zr2−$Cl2^{a}$ vector and the triangular Zr1−$Cl2^{a\text{-}a}$−Zr1 plane generated by intercluster bridging on the chain from 161.3° in $KZr_6Cl_{13}Be$ (Figure 4) to 180° in $Zr_6Cl_{10.5}I_{1.5}B$. In other words, cluster orientations now alternate by precisely 90°, the $Cl2^{a\text{-}a\text{-}a}$ bridges are planar, and, of course, $a = b$, which formerly differed by ∼0.51 Å (0.62 Å in $Zr_6Cl_{13}B$). The two types of $Cl^{i}$ atoms that formerly bridged the Zr1−Zr2 edges in each cluster (Cl4, Cl5) become equivalent in the process, and it is on these sites that random 19.1(3)% iodine substitution acts to elevate the symmetry. (Compare the synopsis illustration of the tetragonal cell.)

The source of the changes brought on when, on average, 1.5 out of 8 $Cl^{i}$ per cluster that bridge Zr1−Zr2 (waist to apex) are substituted by the larger $I^{i}$, clearly a size (matrix) effect, can be readily visualized in Figure 4. The limit to the former buckling of the interchain linkages must be based (at least in major part) on the Cl···Cl closed-shell repulsions. Separations of ∼3.5 Å or less are generally "tight",[2] and examples here are as follows: (a) 3.42 Å for intrachain $Cl1^{i\text{-}i}$−$Cl2^{a\text{-}a\text{-}a}$ in the basal planes, presumably ameliorated by the higher coordination numbers and lower effective charges of these atoms, and (b) the most significant, 3.45 and 3.59 Å interchain between inner Cl3 and the Cl4,5.[28] Only the former value changes significantly (3.45 to 3.56 Å) when the larger iodide forces the formation of the tetragonal phase. (The Cl3 atoms that bridge the short edges of cluster waist and alternate with the interchain linking $Cl2^{a\text{-}a\text{-}a}$ are not visible in the view near the center of Figure 4, but they can be readily discerned in the outer parts of the drawing. Longer interchain separations occur between Cl4 and Cl5, 3.61 and 3.62 Å, and to Cl2, 3.54 and 3.57 Å, respectively.) The larger iodine substituted for Cl4,5 would seem incompatible with the latter distances, but the higher symmetry coupled with expansions makes it possible, particularly 0.55 Å in *a*, 0.08 in *c*, and 0.05 Å for the average $\bar{d}$(Zr−$Cl2^{a\text{-}a\text{-}a}$). The shortest I···Cl contacts are now intrachain to Cl2 (3.57, 3.62 Å) and Cl3 (3.62 Å) and interchain to Cl3 (3.52 Å). A reasonable minimum separation between Cl and I might be the average of their "tight" packing, ∼3.75 Å, but this would apply well only with higher iodine occupancies. The substitution process is presumably continuous, and the symmetry transformation is allowed by Landau theory and second order (or higher).

It is interesting to note that the $Zr_6X_{13}Z$ structure has a close relationship to that of the $Nb_6Cl_{14}$ parent,[6] which is realized in

(28) These separations are probably overestimated using the $KZr_6Cl_{13}Be$ atom parameters and $Zr_6Cl_{13}B$ lattice constants, since the greater disparity between *a* and *b* in the latter indicates a greater twisting of the chain linkages. Also, the substitution of I is presumably correlated on a short range, since neighboring I···I distances otherwise would be 3.75 Å intrachain and 3.72 Å interchain.

**Table 5.** Results of $Zr_6Cl_yI_zB$ Reactions with Different Chlorine/Iodine Proportions

| loaded compn | $y+z$ | chlorine/iodine ($y/z$) | phases found | lattice constants: $a$ and $b$, Å | $c$, Å | $V$, Å$^3$ |
|---|---|---|---|---|---|---|
| $Zr_6Cl_9IB$ | 10 | 9 | $Zr_6Cl_{13-x}I_xB$ | 11.976(2)[a] | 7.480(1) | 1072.9(3) |
| $Zr_6Cl_7IB$ | 8 | 7 | $Zr_6Cl_{13-x}I_xB$ + unknown A (minor) | 12.030(1)[a] | 7.4991(8) | 1085.3(2) |
| $Zr_{>6}Cl_{11.5}I_{1.5}B$ | 13 | 7.5 | $Zr_6Cl_{11.47}I_{1.53}B$ + unknown A | 12.014(2)[a] | 7.494(1) | 1081.7(3) |
| $Zr_6Cl_yI_zB$ | $8 \le y+z \le 14$ | 3.5−1.0 | unknown A only | | | |
| $Zr_6Cl_yI_zB$ | 13 | 0.625 | $Zr_6Cl_xI_{12-x}B$ + unknown A | 14.378(2)[b] | 9.902(2) | 1772.9(7) |
| $Zr_6Cl_3I_{10}B$ | 13 | 0.3 | $Zr_6Cl_xI_{12-x}B$ | 14.4110(9)[b] | 9.928(1) | 1785.5(3) |
| $Zr_6Cl_{1.3}I_{10.7}B$ | 12 | 0.121 | $Zr_6Cl_{1.27}I_{10.73}B$ | 14.389(1)[b] | 9.915(2) | 1777.8(5) |

for comparison:

| | | | | |
|---|---|---|---|---|
| $Zr_6Cl_{13}B$[16] | $a = 11.523(2)$[c] | $b = 12.142(2)$ | $c = 7.4221(9)$ | $V = 1038.4(3)$ |
| $Zr_6I_{12}B$[5] | $a = 14.534(1)$[b] | | $c = 9.986(1)$ | $V = 1825(1)$ |

[a] Primitive tetragonal. [b] Rhombohedral, hexagonal setting. [c] Orthorhombic, *Pnnm*.

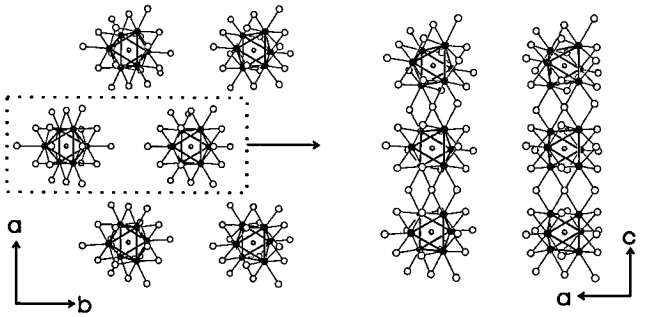


**Figure 6.** Schematic representation of the relationship between clusters in (left) the $Zr_6Cl_{14}B(Nb_6Cl_{14})$ structure ([001] projection on $z = {}^1/_2$) and (right) the $Zr_6Cl_{13}B$ structure ([010] projection on $y = 0$). Translation of every second row of clusters in $Zr_6Cl_{14}B$ by b/2 gives the cluster arrangement in the latter structure (see text).

a stuffed version in many cluster compounds with the general composition $A^IZr_6X_{14}Z$ with X = I, Br, or Cl and Z as one of many main-group or transition-metal interstitials.[1,2] The relationship between the types is shown in Figure 6. The transformation of $Nb_6Cl_{14}$ [$=(Nb_6(Cl^i)_{10}(Cl^{i\text{-}a})_2(Cl^{a\text{-}a})_{4/2}$] into $Zr_6Cl_{13}B$ [$=(Zr_6Cl^i{}_{10}(Cl^{i\text{-}i})_{2/2}(Cl^{a\text{-}a\text{-}a})_{6/3}$] is accomplished by a translation of every other row of clusters in the former along b by $b/2$ and insertion of Z. The two $Cl^{i\text{-}a}$ functions per cluster become two $Cl^i$ and two $Cl^i$ become a single $Cl^{i\text{-}i}$ plus a $Cl^-$ in the channels, while the two $Cl^{a\text{-}a}$ linkages parallel to [001] become $Cl^{a\text{-}a\text{-}a}$. Finally, the 14th lone $Cl^-$ is replaced by a cation in $K^+Zr_6Cl_{13}Be^-$ or nothing in $Zr_6X_{13}B$. The substitutions reported here and the $Zr_6X_{13}Z$ structure also bear some relationship to the effects of mixed halide on the $Nb_6X_{14}$ structure.[9] Substitution of iodide into the somewhat complex bridging motif of $Nb_6Cl_{14}$ (above) converts the orthorhombic parent structure into the more open cubic ($Pa\bar{3}$) $Nb_6(Cl^i)_{12}$-$(I^{a\text{-}a\text{-}a})_{6/3}$, that is, with similar tribridging outer iodides and retention of the cluster layering. Further iodide substitution to produce $Nb_6Cl_{10.8}I_{3.2}$ occurs in the six $Cl^i$ sites that bridge edges of the cluster normal to the $\bar{3}$ axis, quite analogous to the behavior in $Zr_6I_{12-x}Cl_xB$.

**Phase Breadths.** On the basis of the changes reported here, chlorine substitution in the $Zr_6I_{12}C$ structure type on only I2 sites to give $Zr_6(Cl_xI_{6-x})^iI_6Z$ could in principle range over $0 \le x \le 6$, i.e., from $Zr_6I_{12}Z$ to $Zr_6Cl_6I_6Z$. For the $Zr_6Cl_{13}Z$ structure, the corresponding process for $[Zr_6(Cl3^i)_2(Cl_{8-x}I_x)^iCl_2Z]$ could cover $0 \le x \le 8$, that is, from $Zr_6Cl_{13}Z$ to $Zr_6Cl_5I_8Z$, although there does not appear to be room for that much $I^i$ in the structure. (The distinct $Cl3^i$ along the chains are not included in the substitution sites, as these are more restricted by both $Cl^{a\text{-}a\text{-}a}$ and interchain interactions (above).) Some reactions run in the $Zr_6Cl_yI_zB$ system with Cl:I ratios between 9:1 and 0.12:1 to examine the ranges of phase stability are summarized in Table 5. In fact, compositions in the center of the region, ~1.0 < Cl/I ≤3.5, yield another surprise, a third phase (A) that is not yet completely characterized.[13] The $Zr_6X_{13}B$ structure is the only phase at Cl/I = 9, is the major phase (≥90%) at 7.5, and is mixed with "A" in approximately equal amounts at Cl/I = 7.0. A chlorine-rich, 15-e $Zr_6X_{12}B$ phase was not seen although $Zr_6I_{12}B$ is known.[20] The phase width for $Zr_6Cl_{13-x}I_xB$ corresponds to about $0 \le x \le 1.5$, the limit lying close to the crystal analyzed structurally. (The lattice constants may also depend somewhat on reaction temperature.) At the other extreme, the rhombohedral boride is stable to a chlorine limit of about $Zr_6Cl_{1.4}I_{10.6}B$. The three boride structures formed, the two extremes of which are reported here, represent novel ways to adapt size differences to structural constraints. On the other hand, chloride-rich regions with Be as an interstitial yield only the 14-e $Zr_6X_{12}Be$, not the less favorable 13-e $Zr_6X_{13}Be$, with iodine substitution occurring up to about $Zr_6Cl_{8.8}I_{3.2}Be$ ($a$ = 13.430(2) Å, $c$ = 9.165(3) Å, $V$ = 1431.6(6) Å$^3$ vs 13.161(1) Å, 8.840(1) Å, 1324.6 Å$^3$, respectively, for $Zr_6Cl_{12}Be$[20]). Presumably less serious I···I interactions result with the larger Be, and the more rapid increase in $c$ again signals iodide substitution for $Cl2^i$.

**Acknowledgment.** This work was supported by the National Science Foundation, Solid State Chemistry, via Grant DMR-9207361 and was carried out in the facilities of Ames Laboratory, U.S. Department of Energy. M.K. thanks the Alexander von Humboldt Foundation for a Feodor-Lynen Fellowship.

**Supporting Information Available:** Tables giving additional crystallographic details, anisotropic displacement parameters, and bond angles for the three structures (6 pages). Ordering information is given on any current masthead page.

IC950889Y